Vietnam Journal of Science and Technology ***57*** *(5) (2019) 559-571*

doi:10.15625/2525-2518/57/5/13661

PREPARATION AND CHARACTERIZATIONS OF PLASTICIZED PMMA/PVC/$Mg(ClO_4)_2$ ELECTROLYTES

Do Quang Tham[1, *], Tran Thi Mai[1], Thai Hoang[1], Nguyen Thi Kim Dung[2], Nguyen Quang Tung[3], Nguyen Thi Dieu Linh[3], Lai Thi Huyen[3], Dam Xuan Thang[3], Do Van Cong[1], Mai Duc Huynh[1], Nguyen Thi Thai[1]

[1]*Institute for Tropical Technology, VAST, 18 Hoang Quoc Viet, Cau Giay, Ha Noi*

[2]*National Academy of Education Management, 31 Phan Dinh Giot, Thanh Xuan, Ha Noi*

[3]*Faculty of Chemical Technology, HaUI, Tay Tuu, North Tu Liem, Ha Noi*

[*]Email*: dqtham@itt.vast.vn*

Received: 4 March 2019; Accepted for publication: 25 June 2019

Abstract. Electrolyte films based on poly(methyl methacrylate) (PMMA) and poly(vinyl chloride) (PVC) were prepared by using casting method with the addition of 100 wt.% to 240 wt.% of dioctyl phthalate (DOP), propylene carbonate (PC) as plasticizers and $Mg(ClO_4)_2$ as an electrolytic salt. The Fourier infrared spectra (FTIR), tensile, electrical properties, and surface morphology of electrolyte films were investigated. The FTIR spectra of plasticized PMMA/PVC blends indicated that there were secondary interactions between plasticizers and PMMA/PVC matrix. There were also molecular interactions between $Mg(ClO_4)_2$ and the blends, which indicated that $Mg(ClO_4)_2$ was well dissolved and solvated in the blends. Tensile results showed that $Mg(ClO_4)_2$ improved the elongation at break and the reduced tensile strength and Young's modulus of the blends due to this salt can act as an internal lubricant for the blends. The SEM and EDX-mapping micrographs showed the wrinkled surface morphology of the electrolyte film, all raw materials were dispersed regularly into each others at molecular and ionic levels. For the electrolytes containing 10 wt.% of $Mg(ClO_4)_2$, the ionic conductivity increased with increasing plasticizer content and achieved in the range of $1.80 \times 10^{-4} \div 1.03 \times 10^{-3}$ (S/cm). For the electrolyte containing 200 wt.% of the plasticizer, the ionic conductivity increased with increasing magnesium salt content and achieved in the range of $2.31 \times 10^{-4} \div 4.57 \times 10^{-3}$ (S/cm).

Keywords: polymer electrolytes, PMMA, PVC, magnesium perchlorate, ionic conductivity.

Classification numbers: 2.9.3, 2.5.2, 2.2.2.

1. INTRODUCTION

Currently, polymer electrolytes are considered as one of the most promising materials for applications in electrochemical devices, such as: rechargeable batteries, fuel cells, super capacitors [1]. Gel polymer electrolytes are ionic conductive materials, which are often made by introducing electrolytic salts into a suitable polymer matrix in the presence of plasticizers by different methods [2, 3]. Many types of polymers have been employed for gel polymer

electrolytes such as: poly(ethylene oxide) or polyethylene glycol [4, 5], poly(methyl methacrylate) (PMMA) [6], methyl ether methacrylate [7], polyacrylonitrile [8], polyvinyl chloride (PVC) [9], and poly(vinylidene fluoride-co-hexafluoropropylene) [10]. PMMA has been previously used as a polymer host for plasticized electrolytes [11-13]. However, the gel-like properties made the PMMA based electrolytes was not able to form free-standing film at high level of plasticizer. Therefore, there are some studies reported the blending of PMMA with other polymers, among them PVC has been more often used for improving mechanical strength of plasticized PMMA gel electrolytes [14-16].

As mentioned above, polymer gel electrolytes have been applied for lithium battery electrolytes and thus can also adopted for rechargeable magnesium batteries [17]. Nevertheless, as far as we know, there is no any report on gel polymer electrolytes based on plasticized PMMA/PVC with magnesium salts. Therefore, in this paper, we report. a study on preparation and characteristics of electrolyte films based on PMMA, PVC, plasticizers and magnesium perchlorate salt. The Fourier transform infrared (FTIR) spectroscopy, electrical conductivity, tensile properties and surface morphology of electrolyte films were investigated, the obtained results were also reported and discussed.

2. EXPERIMENTAL

2.1. Materials

Polyvinyl chloride (PVC, SG-660, k index of 65-67) was supplied by Plastic & Chemical Corp., Ltd., (TPC Vina, Vietnam). Ethyl alcohol (ethanol, 99.7 %), methyl alcohol (methanol, 99.7 %), dioctyl phthalate (DOP, 95 %) were provided by Duc Giang Chemical and Detergent powder Joint Stock Company, Viet Nam. PMMA (M_W = 120000), propylene carbonate (PC, 99.7 %) were purchased from Aldrich (USA). Tetrahydrofuran (THF, 99.7 %) and $Mg(ClO_4)_2$ are analytical grade products of Xilong Co., Ltd., China. $Mg(ClO_4)_2$ powder was dried in a vacuum oven at 120 °C for 24 h and stored in a sealed glass bottle before use. Other chemicals were used as received without further purification.

2.2. Preparation of samples

The electrolyte films were prepared by dissolving the polymers, plasticizers and $Mg(ClO_4)_2$ with predetermined amounts as indicated in Table 1 in THF for 2 hours. Solutions with predetermined weights were then cast onto release paper as films, so that the thickness and area of dried films were about 0.2 mm and 50 cm^2, respectively. Evaporation of THF solvent was allowed at room temperature in a fume hood for 24 hours, followed by drying in vacuum oven at 40 °C for 24 hours. All samples were stored in a desiccator before testing.

2.3. Characterizations

The tensile properties including the Young's modulus (YM), tensile strength (TS) and elongation at break (EB) of electrolyte films were conducted using Zwick Tensile V.2.5 Machine (Germany) with crosshead speed of 50 mm/min, according to ASTM D882 for thin plastic films.

The FTIR spectra of electrolyte films were recorded using a Nicolet/Nexus 670 Fourier Transform Infrared spectrometer (USA) in the wave region between 4000 and 400 cm^{-1} at 4 cm^{-1} resolution and 32 scan signal averaging, at room temperature.

The surface morphology of electrolyte films was observed using a Scanning Electron Microscope (SEM, JSM-6510LV JEOL, Japan) combined with Energy Dispersive X-ray (EDX) spectroscopy and elemental mapping technique at electron acceleration voltage of 15 kV. The films were coated with a platinum layer before morphology testing.

The AC conductivity (σ_{AC}) and AC impedances (real part - Z' and imaginary part - Z") of electrolyte films were measured by using an Agilent E4980A precision RLC meter and 16451B test fixture as described in Scheme 1, the electrodes are all made from stainless steel, according to the literature [18], in the frequency range of 25 Hz ÷ 1 MHz, with peak amplitude of 1.0 V and applied voltage to the reference electrode of 0 V.

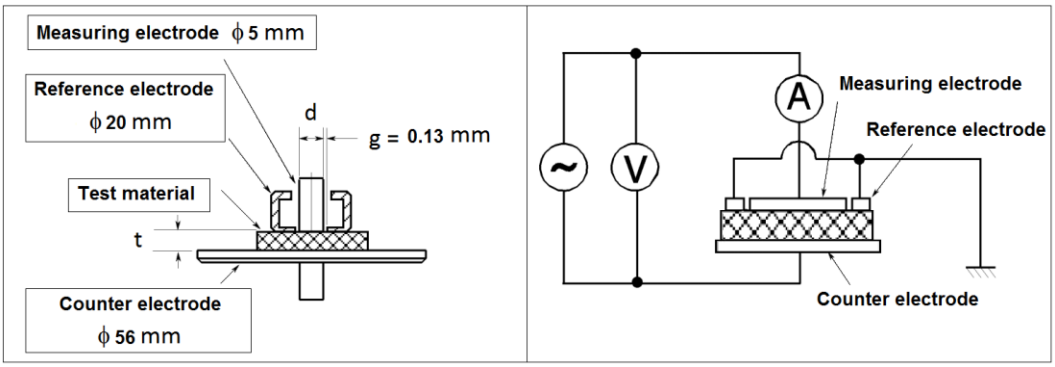

Scheme 1. Three-electrode system of the 16451B and block diagram for AC conductivity measurement.

DC conductivity of electrolyte films was evaluated using a three-electrode test fixture and a TR-8401 electrometer (Takeda Riken, Japan), DC applied voltage of 1.0 V. The electrode system and DC conductivity measurement system are similar to Scheme 1, but diameters of measuring, guard and unguarded electrodes are of 50, 70 and 100 mm, respectively.

Table 1. Compositions used for the preparation of plasticized PMMA/PVC electrolyte films.

Sample code	PMMA (g)	PVC (g)	DOP (g)	PC (g)	$Mg(ClO_4)_2$ (g)	THF (g)
P100	0.45	0.45	0.45	0.45	-	5.1
P160	0.45	0.45	0.72	0.72	-	5.1
P200	0.45	0.45	0.90	0.90	-	5.1
P240	0.45	0.45	1.08	1.08	-	5.1
P100.10	0.45	0.45	0.45	0.45	0.200	5.1
P160.10	0.45	0.45	0.72	0.72	0.260	5.1
P200.10	0.45	0.45	0.90	0.90	0.300	5.1
P240.10	0.45	0.45	1.08	1.08	0.340	5.1
P200.10	0.45	0.45	0.90	0.90	0.300	5.1
P200.20	0.45	0.45	0.90	0.90	0.450	5.1
P200.30	0.45	0.45	0.90	0.90	0.771	5.1
P200.40	0.45	0.45	0.90	0.90	1.200	5.1

3. RESULTS AND DISCUSSION

3.1. The tensile properties of plasticized PMMA/PVC/$Mg(ClO_4)_2$ electrolyte films

Table 2 presents the results of tensile properties of plasticized PMMA/PVC blends and plasticized PMMA/PVC/$Mg(ClO_4)_2$ electrolyte films with the compositions as shown in Table 1. The results show that when increasing plasticizer content from 100 to 240%, the YM of PMMA/PVC (1:1) blend strongly reduces from 15.08 MPa down to 1.32 MPa and the TS of blend reduces from 3.81 MPa down to 0.68 MPa, and the strong decrease in TS is observed with the P200 and P240 samples (from 1.15 MPa to 0.68 MPa). Meanwhile, the EB of blends slightly increases from 46% to 61%. These variations of tensile properties of the blend are due to the introduction of plasticizers into PMMA/PVC blends. The plasticizer molecules can penetrate between the polymeric chains to form secondary bonds which reduce the molecular interactions between polymer chains (PVC-PVC, PMMA-PVC and PMMA-PMMA), thus, the EB of PMMA/PVC blends increases, while their TS and YM values decrease [19, 20].

For the electrolyte films containing 10 wt.% of $Mg(ClO_4)_2$, the TS and YM of the electrolyte films strongly decrease. Meanwhile, their EB increase significantly in comparison with the neat plasticized samples, it reaches a maximum value (195% for P200.10 sample) and then tends to decrease when higher plasticizer content was introduced (121% for P240.10 sample). It has been reported that $Mg(ClO_4)_2$ with low molecular weight can be soluble in the plasticizers inside the blends [21], therefore, it can act as an internal lubricant for the blends and facilitates the flow ability of polymer chains under tensile force, leading to the remarkable improvement of EB of the blends.

Table 2. Tensile properties of the plasticized PMMA/PVC electrolyte film without $Mg(ClO_4)_2$.

Sample codes	Young's modulus (YM, MPa)	Elongation at break (EB, %)	Tensile strength (TS, MPa)
P100	15.08	46	3.81
P160	8.72	55	1.72
P200	1.75	58	1.15
P240	1.32	61	0.68
P100.10	0.81	142	0.83
P160.10	0.40	189	0.65
P200.10	0.36	195	0.48
P240.10	0.23	121	0.30
P200.10	0.36	195	0.48
P200.20	0.34	178	0.40
P200.30	0.26	94	0.22
P200.40	0.23	90	0.20

In comparison with P200.10 sample, the TS, YM and EB of P200/$Mg(ClO_4)_2$ are all decreased by increasing salt contents from 20 to 40 wt.% (compared to total weight). It is interesting to know that the EB of the electrolyte films containing magnesium salt are all higher than that of P200 sample.

3.2. The FTIR spectra of plasticized PMMA/PVC/$Mg(ClO_4)_2$ electrolyte films

Figure 1 shows the FTIR spectra of pure PC, DOP, $Mg(ClO_4)_2$ and two selected electrolyte films, which are P200, P200.10 (with 10 wt.% $Mg(ClO_4)_2$). The FTIR spectrum of pure DOP shows some remarkable characteristic bands: $CH_{(1, 2, 3)}$ stretching vibrations (ν) in the region from 2800 to 3000 cm^{-1}, ν(C=O) at 1728 cm^{-1}, ν(C-C) of aromatic ring at 1600 cm^{-1} and 1581 cm^{-1}. The FTIR spectrum of PC also shows its characteristic bands: ring deformation (δ) band at 777 cm^{-1}, ν(C-O) at 1791 cm^{-1}. In the spectrum of $Mg(ClO_4)_2$, the peaks at 1145, 1112, 1089 cm^{-1} are assigned for ν(ClO) vibration modes and the peak at 627 cm^{-1} is assigned for asymmetric bending (δ_{as}) of ClO_4 tetrahedrals [15, 22-25]. It is experienced that PC and $Mg(ClO_4)_2$ can absorb moisture from air when loading samples into FTIR instrument [19, 26]. Therefore, strong absorption bands in the region of 3000 - 3600 cm^{-1} and the bands at 1634 cm^{-1} are observed in their FTIR spectra (Figure 1b, 1c).

Referring to our previous study, three ν(C-Cl) vibration modes of pure PVC were reported, appearing at 692, 636 and 614 cm^{-1} [27]. In this study, only two vibration modes of ν(C-Cl) at 637 and 616 cm^{-1} in spectra of P200 sample are observed, the next peak (at 651 cm^{-1}) is attributed to aromatic ring bending (r_{ing}) of DOP. The vibration band of ν(C=O) in the region 1700-1808 cm^{-1} is widened, in addition, the band of ν(C=O) and δ(C=O) are shifted to higher wavenumber (at 1732 and 747 cm^{-1}) in comparison with that of DOP (1728 and 743 cm^{-1}). This shift also happens with δ(C=O) of PC in spectra of P200 sample (1791 cm^{-1} and 1808 cm^{-1} for pure PC and P200 samples, respectively). In our previous study, the strong hydrogen bonds and polar interactions between PMMA-PMMA, PMMA-PVC and PVC-PVC macromolecules were elucidated by FTIR study. In this case, the introduction of DOP and PC molecules screens and weakens the polar interaction and hydrogen bonds between polymer chains. Also, secondary polar interactions between the plasticizers and the polymers have been formed, therefore, the materials become more flexible.

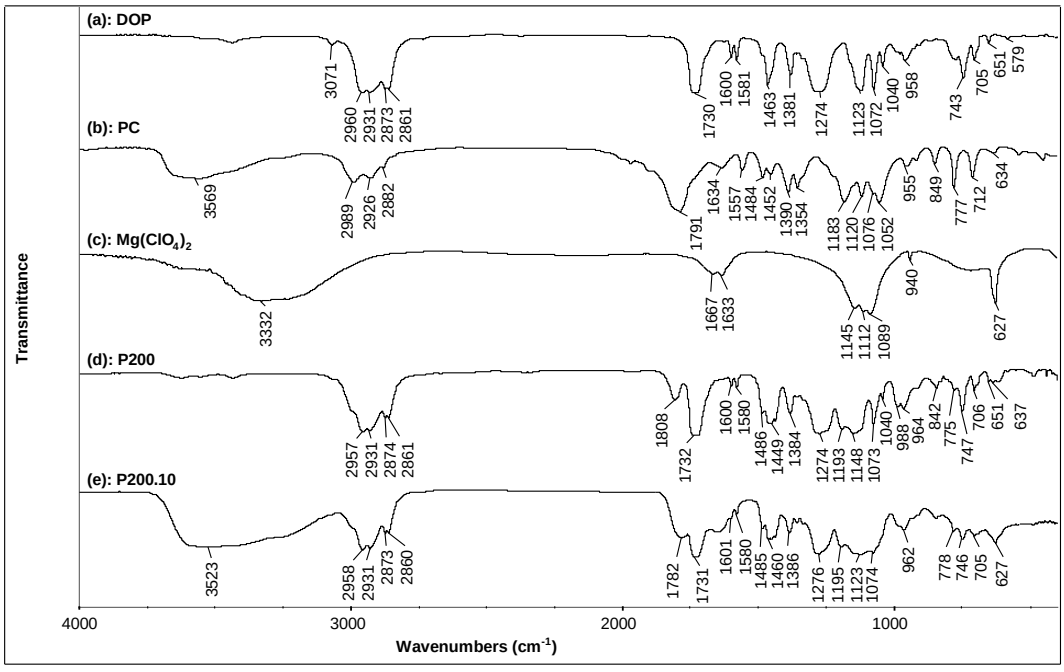

Figure 1. FTIR spectra of (a): pure DOP; (b): pure PC; (c): pure $Mg(ClO_4)_2$; and the electrolyte films of (d): P200, (e): P200.10.

In the FTIR spectrum of P200.10 (Figure 1e), there are some different absorption bands compared with the spectrum of P200. The first difference is the strong absorption band in the 3000-3600 cm^{-1} due to moisture absorbed on surface of the P200.10 electrolyte film. The second one is the shift to lower wavenumber of ν(C=O) at 1782 cm^{-1}, in accordance with the widened absorption band of ν(C=O) from 1700-1782 cm^{-1}, which may arise from the strong molecular interaction between $Mg(ClO_4)_2$ and the plasticizers such as: Mg^{2+} with O=C-O groups of PC, DOP and PMMA. The third one is the appearance of a single and wide peak at 627 cm^{-1}, instead of 3 peaks at 657 (δ_{ring}), 637, 616 cm^{-1} (ν(C-Cl) as shown in Figure 1.d. The reason can be explained by the overlap of the two absorption bands: ν(ClO_4) of paired and free $(ClO_4)^-$ ions and ν(C-Cl) of PVC. In addition, the solvation of $Mg(ClO_4)_2$ in the plasticizer and polymer matrices (PMMA, PVC) may contribute to the peak widening at 627 cm^{-1}. It is worthy to note that $Mg(ClO_4)_2$ is more soluble in PC than DOP, however, DOP is more often used as a plasticizer for PVC. That is the reason why both DOP and PC are used in this study.

3.3. The morphology of plasticized PMMA/PVC/$Mg(ClO_4)_2$ electrolyte films

Figure 2 displays the SEM micrographs of the plasticized PMMA/PVC (P200) film and the P200.20 electrolyte film (with 20 wt.% of $Mg(ClO_4)_2$ over total weight of the electrolyte sample). It can be seen the wrinkles on the surface of the P200, P200.20 films, which are caused by the high flexibility of the films and the random deformations of the material when the THF solvent was evaporated. In comparison, the surface morphology of P200.20 sample is more smooth. This indicates that $Mg(ClO_4)_2$ has lessen the driving force for the deformation of plasticized PMMA/PVC film due to the high solubility of $Mg(ClO_4)_2$ into plasticizers at ionic and molecular levels [15].

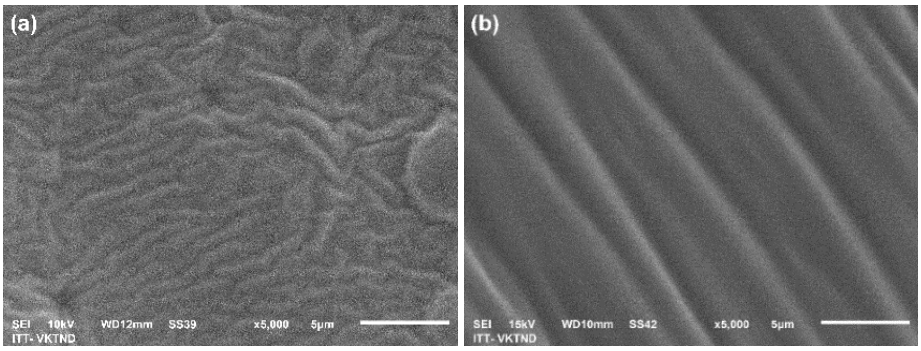

Figure 2. SEM micrographs of (a): plasticized PMMA/PVC (P200) film and (b): P200.20 electrolyte film (with 20 wt.% of $Mg(ClO_4)_2$).

Figure 3 shows (a): the origin SEM micrograph of P200.20 film and elemental mapping of (b): oxygen; (c): chlorine and (d): magnesium using SEM/EDX technique. Figure 3a also shows the wrinkled morphology on the surface of P200.20 films. Nevertheless, uniform distribution of chlorine and magnesium in the investigated area of the sample can be easily observed. In Figure 3b, an area with high concentrated dots is detected, that may be attributed to the oxygen of PMMA phase. This indicates that the wrinkles are not interface of PMMA and PVC phases, because at these wrinkles, there are all elements appeared with relatively uniform distribution. It can be suggested that magnesium salt is regularly dispersed in the plasticized PMMA/PVC matrix at ionic and molecular levels.

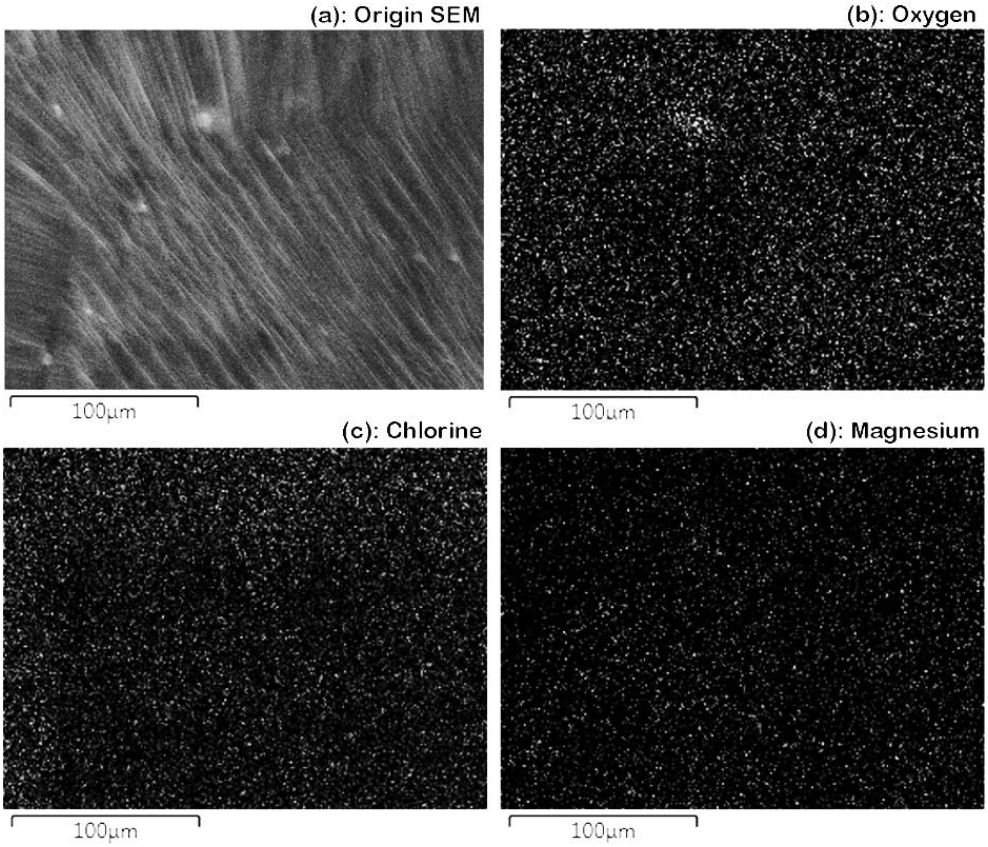

Figure 3. (a): Origin SEM micrograph of P200.20 film; and elemental mapping of (b): Oxygen atoms; (c): Chlorine atoms; and (d): Magnesium atoms on surface layer of the film.

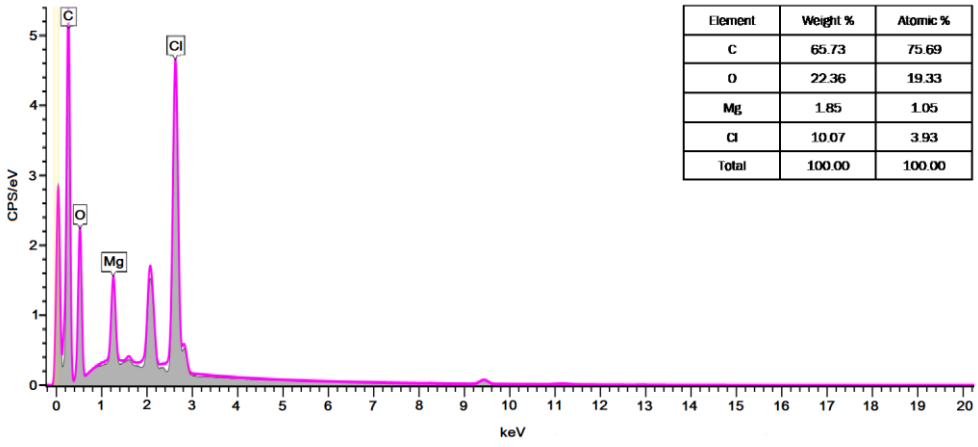

Element	Weight %	Atomic %
C	65.73	75.69
O	22.36	19.33
Mg	1.85	1.05
Cl	10.07	3.93
Total	100.00	100.00

Figure 4. EDX spectrum of P200.20 electrolyte film and the table of compositions at right comer.

Figure 4 presents the EDX spectrum of P200.20 electrolyte film and the table included (at right corner) shows the qualitative elemental analysis on the surface of the electrolyte film. The peaks of major elements such as C, O, Mg and Cl are all appeared. The detectable concentrations of these elements are showed in Table 3, where weight percentages are in ascending order as: C (65.37 %) > O (22.36 %) > Cl (10.07 %) > Mg (1.85 %). Supposing that all raw materials are

regularly distributed, the weight percentages of the P200.20 sample can be calculated as: C (48.20 %) > O (34.69 %) > Cl (14.79 %) > Mg (2.31 %). This comparison indicates that magnesium ions are appeared on the surface of the electrolyte films with lower concentration than those in the bulk, however, it may be within the acceptable margins of error.

3.4. The electrical properties of plasticized PMMA/PVC/$Mg(ClO_4)_2$ electrolyte films

The Figure 5 depicts the variations of AC conductivity of the electrolyte films with and without $Mg(ClO_4)_2$ as functions of frequency. It can be observed that AC conductivity of all samples increases with frequency, because at low frequencies, conductivity is only contributed by the flow of free electrons and/or ions. When frequency increases, contributions of ionic, electronic and electrode polarizations are increased, which causes higher displacement current "flowing" in electrolytes [28]. At low frequency region, the low conductivity of P100 and P200 blends ($2.7\times10^{-11} \div 3.1\times10^{-10}$ S/cm at 25 Hz) is attributed to the very low concentration of free electrons in the films. However, by adding 10 wt.% of $Mg(ClO_4)_2$ electrolytic salt, the AC conductivities of the P100.10 and P200.10 electrolyte films ($1.0\times10^{-8} \div 6.0\times10^{-8}$ S/cm at 25 Hz) are strongly higher than those of P100 and P200 blend films. Figure 5a indicates that those increments in conductivities of the P100.10 and P200.10 electrolyte films compared with that of P100 and P200 blend films are attributed to ionic conduction of $Mg(ClO_4)_2$ electrolytic salt. In other words, this elucidates the ionic conductivity of electrolyte films containing $Mg(ClO_4)_2$ salt.

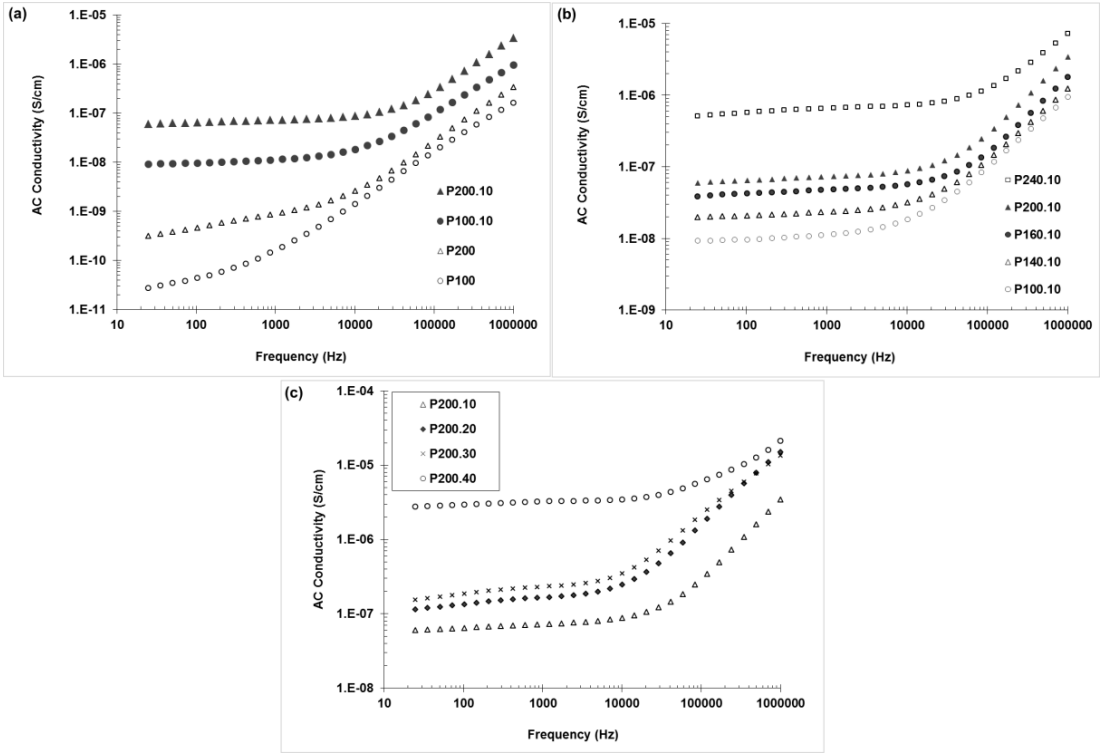

Figure 5. The AC conductivity of electrolyte films with and without of $Mg(ClO_4)_2$.

Figure 5b also shows that the conductivities of electrolyte films containing the same 10 wt.% of $Mg(ClO_4)_2$ increase with increasing the plasticizer contents, because plasticizers can improve the solubility and solvation of the salt, thus, increasing mobility of Mg^{2+} and $(ClO_4)^-$

ions. Figure 5c indicates that the conductivities of electrolyte films increase with increasing $Mg(ClO_4)_2$ salt contents from 10 to 40 wt.%. However, it should be noted that the higher salt content causes the lower mechanical properties of electrolyte films.

Figure 6a (the left) and 6b (the right) depict the plots of complex impedance components (Z' and Z") of plasticized PMMA/PVC/$Mg(ClO_4)_2$ electrolyte films with the variation of plasticizer and magnesium salt contents, respectively. The schema of equivalent circuit for the electrolyte-electrode system is also depicted inside Figure 6a, where R_b is the bulk resistance of gel electrolyte film; R_{ct} and C_p are the charge transfer resistance and capacitance of electrolyte film, respectively, Z_w is interfacial impedance related to some processes at low frequency region [19, 25, 29]. It can be observed that the experimental points (unfilled legends like □, △, ○) can be fitted well with semicircles (the dash curves) in high and middle frequency regions, which are related to R_{ct} and C_p components. The experiment points of the tails at low frequency region, which are attributed to the interfacial impedance (Z_w), do not lie on these semicircles. When completing the semicircles, the total of resistances ($R_x = R_{ct} + R_b$) of electrolyte-electrode system and bulk resistance (R_b) can be evaluated by the intercepts of the semicircles with real part axis at low and high frequency regions, respectively [30]. For more accurate calculation, R_b values were evaluated via linear extrapolation from the last three points at highest frequencies. R_{ct} and ionic conductivity (σ_{ion}) of electrolyte film can be determined as: $R_{ct} = R_x - R_b$; $\sigma_{ion} = (t/A)\times(1/R_b)$, where t is thickness of sample, A is area of measuring electrode [31, 32]. Figure 6 shows that the radius of the Z'-Z" fitted semicircle (or R_{ct}) of the complex impedance plot is reduced by increasing plasticizer content as well as increasing magnesium salt content. The evaluations of R_b, R_{ct} and calculated electrical conductivities of electrolyte films are shown in Table 3. For comparison, the results of DC conductivity measurement of electrolyte films are also represented.

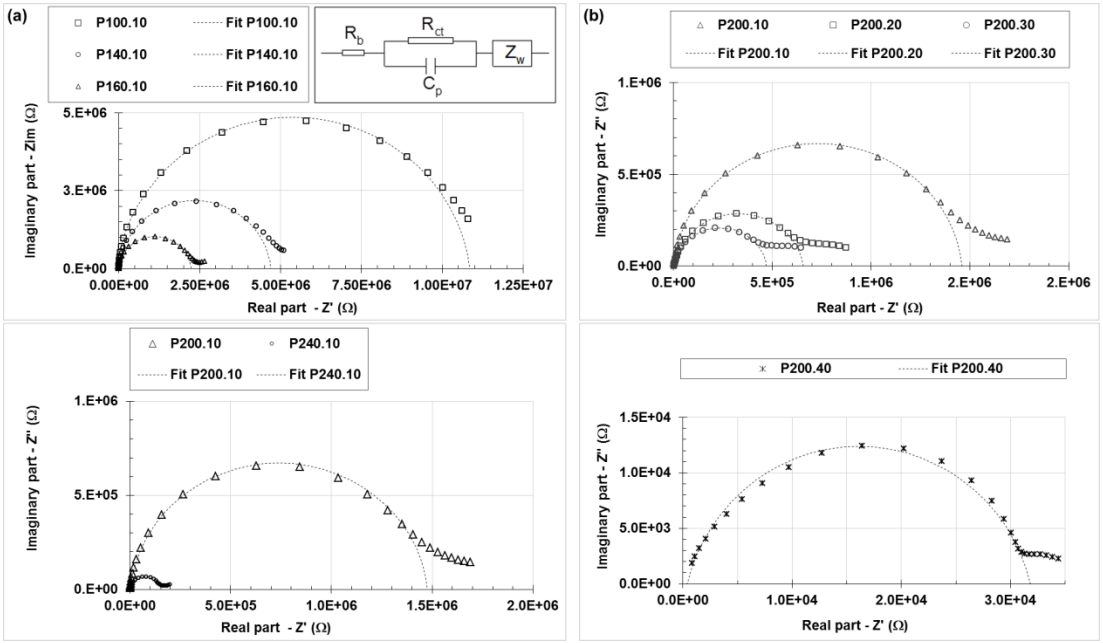

Figure 6. Impedance plot of (a): electrolyte films containing 10 wt.% of $Mg(ClO_4)_2$ with different plasticizer contents (the left); (b): electrolyte films containing different $Mg(ClO_4)_2$ contents and same 200 wt.% of plasticizers (the right).

Table 3 shows that ionic conductivity as well as AC conductivity at 25 Hz of the electrolytes increase with increasing plasticizer and magnesium salt contents. The lower values of DC conductivity compared to AC conductivity may be due to the formation of polarization layers near the electrodes, which restrict the directed movement of ions. The conductivity enhancement of plasticizer can be explained by the better dissociation of electrolytic salt at the higher concentration of plasticizer and salt itself [20]. It is also reported that the higher dielectric constant of plasticizer results in stronger enhancement of electrical conductivity of gel polymer electrolytes. In our case, dielectric constant of PC is much higher (ε' = 64.9) [20] than those of PMMA, PVC and DOP (about 3-5) [31]. With the PC:DOP ratio of 1:1, the ionic conductivity of plasticized PMMA/PVC/$Mg(ClO_4)_2$ electrolyte can achieve 4.57×10^{-3} (S/cm) at the highest investigated magnesium content of 40 wt.%.

Table 3. The evaluated results of R_b, R_{ct}, ionic conductivity (σ_{ion}), DC conductivity and AC conductivity (at 25 Hz) and of plasticized PMMA/PVC/$Mg(ClO_4)_2$ electrolyte films.

Samples	R_b **(Ω)**	σ_{ion} **(S/cm)**	R_{ct} **(Ω)**	σ_{AC} **at 25 Hz (S/cm)**	σ_{DC} **(S/cm)**
P100.10	565.9	1.80×10^{-4}	1.09×10^{7}	9.22×10^{-9}	3.02×10^{-9}
P140.10	507.1	2.01×10^{-4}	4.70×10^{6}	1.97×10^{-8}	8.05×10^{-9}
P160.10	477.1	2.13×10^{-4}	2.23×10^{6}	3.82×10^{-8}	1.57×10^{-8}
P200.10	441.6	2.31×10^{-4}	1.46×10^{6}	5.98×10^{-8}	2.90×10^{-8}
P240.10	98.90	1.03×10^{-3}	1.54×10^{5}	5.07×10^{-7}	1.24×10^{-7}
P200.10	441.6	2.31×10^{-4}	1.46×10^{6}	5.98×10^{-8}	4.10×10^{-8}
P200.20	354.6	2.87×10^{-4}	6.56×10^{5}	1.15×10^{-7}	1.41×10^{-8}
P200.30	36.00	2.83×10^{-4}	4.71×10^{5}	1.54×10^{-7}	1.98×10^{-8}
P200.40	22.30	4.57×10^{-3}	3.15×10^{4}	2.27×10^{-6}	3.02×10^{-7}

4. CONCLUSIONS

The mechanical, electrical properties, infrared spectra and surface morphology of electrolyte films based on plasticized PMMA/PVC containing $Mg(ClO_4)_2$ have been investigated. Plasticizers strongly reduced Young's modulus (YM) and tensile strength (TS), but improved elongation at break (EB) of the electrolytes. $Mg(ClO_4)_2$ also made reducing YM and TS, but significantly made increasing the EB of the electrolytes. The analysis of FTIR spectra, SEM micrographs and EDX indicated that $Mg(ClO_4)_2$ can be dissolved and solvated well in the plasticizer and polymer matrices. The ionic conductivity of electrolyte films has been achieved from 10^{-4} to 10^{-3} (S/cm) and increased with plasticizer and $Mg(ClO_4)_2$ contents.

Acknowledgements: This work is completed under the financial support from the Vietnam National Foundation for Science and Technology Development (NAFOSTED) under grant number 104.02-2018.03. The authors also thank the Vietnam Academy of Science and Technology for a partial financial support.

REFERENCES

1. Wang Y., and Zhong W.-H. - Development of Electrolytes towards Achieving Safe and High-Performance Energy-Storage Devices: A Review, Chem. Electro. Chem. **2** (1) (2015) 22-36.
2. Su'ait M. S., Rahman M. Y. A., and Ahmad A. - Review on polymer electrolyte in dye-sensitized solar cells (DSSCs), Solar Energy **115** (2015) 452-470.
3. Bucur C. B., in: C.B. Bucur, (Ed.) - Challenges of a Rechargeable Magnesium Battery: A Guide to the Viability of this Post Lithium-Ion Battery, Springer International Publishing, Cham, 2018, pp. 11-38.
4. Ren Y., Zhang Z., Fang S., Yang M., and Cai S. - Application of PEO based gel network polymer electrolytes in dye-sensitized photoelectrochemical cells, Solar Energy Materials and Solar Cells **71** (2) (2002) 253-259.
5. James J., Kyung Mo S., Vittal R., Whasup L., and Kang-Jin K. - Quasi-solid-state dye-sensitized solar cells with siloxane poly(ethylene glycol) hybrid gel electrolyte, Semiconductor Science and Technology **21** (5) (2006) 697.
6. Lan J. L., Wang Y. Y., Wan C. C., Wei T. C., Feng H. P., Peng C., Cheng H. P., Chang Y. H., and Hsu W. C. - The simple and easy way to manufacture counter electrode for dye-sensitized solar cells, Current Applied Physics **10** (2, Supplement) (2010) S168-S171.
7. Bella F., Ozzello E. D., Bianco S., and Bongiovanni R. - Photo-polymerization of acrylic/methacrylic gel–polymer electrolyte membranes for dye-sensitized solar cells, Chemical Engineering Journal **225** (1 June) (2013) 873-879.
8. Taslim R., Rahman M. Y. A., Salleh M. M., Umar A. A., and Ahmad A. - Fabrication of a nanoparticle TiO_2 photoelectrochemical cell utilizing a solid polymeric electrolyte of PAN–PC–$LiClO_4$, Ionics **16** (7) (2010) 639-644.
9. Rahman M. Y. A., Salleh M. M., Talib I. A., and Yahaya M. - Light intensity and temperature dependence on performance of a photoelectrochemical cells of ITO/TiO_2/PVC-$LiClO_4$/graphite, Ionics **13** (4) (2007) 241-244.
10. Kim J. Y., Kim T. H., Kim D. Y., Park N.-G., and Ahn K.-D. - Novel thixotropic gel electrolytes based on dicationic bis-imidazolium salts for quasi-solid-state dye-sensitized solar cells, Journal of Power Sources **175** (1) (2008) 692-697.
11. Appetecchi G. B., Croce F., and Scrosati B. - Kinetics and stability of the lithium electrode in poly(methylmethacrylate)-based gel electrolytes, Electrochimica Acta **40** (8) (1995) 991-997.
12. Feuillade G., and Perche P. - Ion-conductive macromolecular gels and membranes for solid lithium cells, Journal of Applied Electrochemistry **5** (1) (1975) 63-69.
13. Zhou Y. F., Xie S., Ge X. W., Chen C. H., and Amine K. - Preparation of rechargeable lithium batteries with poly(methyl methacrylate) based gel polymer electrolyte by in situγ-ray irradiation-induced polymerization, Journal of Applied Electrochemistry **34** (11) (2004) 1119-1125.
14. Stephan A. M., Renganathan N. G., Kumar T. P., Thirunakaran R., Pitchumani S., Shrisudersan J., and Muniyandi N. - Ionic conductivity studies on plasticized PVC/PMMA blend polymer electrolyte containing $LiBF_4$ and $LiCF_3SO_3$, Solid State Ionics **130** (1) (2000) 123-132.

15. Stephan A. M., Kumar T. P., Renganathan N. G., Pitchumani S., Thirunakaran R., and Muniyandi N. - Ionic conductivity and FT-IR studies on plasticized PVC/PMMA blend polymer electrolytes, Journal of Power Sources **89** (1) (2000) 80-87.
16. Rhoo H. J., Kim H. T., Park J. K., and Hwang T. S. - Ionic conduction in plasticized PVC/PMMA blend polymer electrolytes, Electrochimica Acta **42** (10) (1997) 1571-1579.
17. Mohtadi R., and Mizuno F. - Magnesium batteries: Current state of the art, issues and future perspectives, Beilstein Journal of Nanotechnology **5** (2014) 1291-1311.
18. Keysight-Technologies, - Accessories Catalog for Impedance Measurements, Published in USA, 2017.
19. Stephan A. M., Thirunakaran R., Renganathan N. G., Sundaram V., Pitchumani S., Muniyandi N., Gangadharan R., and Ramamoorthy P. - A study on polymer blend electrolyte based on PVC/PMMA with lithium salt, Journal of Power Sources **81** (1999) 752-758.
20. Luqman M. - Recent Advances in Plasticizers, InTech, Rijeka, Croatia, 2012.
21. Vondrák J., X, Sedlařı, X, Ková M., Velická J., Klápště B., Novák V., X, Tězslav, and Reiter J. - Gel polymer electrolytes based on PMMA, Electrochimica Acta **46** (13) (2001) 2047-2048.
22. Wang K., Zeng D., Zhang J. G., Cui Y., Zhang T. L., Li Z. M., and Jin X. - Controllable explosion: fine-tuning the sensitivity of high-energy complexes, Dalton Transactions **44** (28) (2015) 12497-12501.
23. Wu Z., Wang A., and Ling Z. - Spectroscopic study of perchlorates and other oxygen chlorides in a Martian environmental chamber, Earth and Planetary Science Letters **452** (2016) 123-132.
24. [24]. Chen Y., Zhang Y.-H., and Zhao L.-J. - ATR-FTIR spectroscopic studies on aqueous $LiClO_4$, $NaClO_4$, and $Mg(ClO_4)_2$ solutions. Physical Chemistry Chemical Physics **6** (3) (2004) 537-542.
25. Pandey G. P., Agrawal R. C., and Hashmi S. A. - Magnesium ion-conducting gel polymer electrolytes dispersed with nanosized magnesium oxide, Journal of Power Sources **190** (2) (2009) 563-572.
26. Guduru K. R., and Icaza C. J. - A Brief Review on Multivalent Intercalation Batteries with Aqueous Electrolytes, Nanomaterials **6** (3) (2016) 41; doi:10.3390/nano6030041.
27. Tham D. Q., Mai T. T., Hoang T., Trang N. T. T., Chinh N. T., and Thang D. X. - Preparation and FTIR studies of PMMA/PVC polymer blends, PVC-g-PMMA graft copolymers and evaluating graft content, Vietnam Journal of Science and Technology **57** (1) (2019) 32-41.
28. Khamzin A., Popov I. I., and Nigmatullin R. - Correction of the power law of ac conductivity in ion-conducting materials due to the electrode polarization effect, Physical Review E **89** (2014) 032303-1 - 032303-8.
29. Osman Z., Zainol N. H., Samin S. M., Chong W. G., Md Isa K. B., Othman L., Supa'at I., and Sonsudin F. - Electrochemical Impedance Spectroscopy Studies of Magnesium-Based Polymethylmethacrylate Gel Polymer Electroytes, Electrochimica Acta **131** (2014) 148-153.

30. Chia C. H., Chan C. H., and Thomas S. - Functional polymeric composites: Macro to nanoscales, Chapter 5, CRC Press, 2017, pp. 97-129.
31. Ramesh S., and Liew C.-W. - Dielectric and FTIR studies on blending of [xPMMA–(1−x)PVC] with LiTFSI, Measurement **46** (5) (2013) 1650-1656.
32. Anilkumar K. M., Jinisha B., Manoj M., and Jayalekshmi S. - Poly(ethylene oxide) (PEO) – Poly(vinyl pyrrolidone) (PVP) blend polymer based solid electrolyte membranes for developing solid state magnesium ion cells, European Polymer Journal **89** (2017) 249-262.